

The Connection between Spin Wave Polarization and Dissipation

Yutian Wang (王昱天),¹ Jiongjie Wang,¹ Ruoban Ma,¹ and Jiang Xiao (萧江)^{1,2,3,4,*}

¹Department of Physics and State Key Laboratory of Surface Physics, Fudan University, Shanghai 200433, China

²Institute for Nanoelectronics Devices and Quantum Computing, Fudan University, Shanghai 200433, China

³Shanghai Research Center for Quantum Sciences, Shanghai 201315, China

⁴Shanghai Branch, Hefei National Laboratory, Shanghai 201315, China

This study establishes a fundamental connection between the dissipation and polarization of spin waves, which are often treated as independent phenomena. Through theoretical analysis and numerical validation, we demonstrate that within the linearized spin wave regime, a spin wave mode's dissipation rate, defined as the ratio of linewidth to the resonance frequency, exceeds Gilbert damping by a factor given by its spatially averaged polarization. This average is governed by a non-positive definite weight, whose magnitude depends on the magnon density of the local excitation, while its sign is dictated by the local polarization handedness. Remarkably, this universal connection applies across diverse magnetic interactions and textures, offering crucial insights into spin wave dynamics and dissipation.

Spin waves, or magnons in quantized form, are collective excitations of magnetic moments in magnetic materials [1]. The study of spin waves bridges fundamental physics with practical applications, from understanding magnetic phase transitions to developing novel spintronic devices [2]. Similar to sound waves transmitting energy through vibrations, spin waves carry magnetic energy and angular momentum without the transport of charge. This unique property has made them increasingly attractive for next-generation information processing technologies with reduced energy consumption and faster processing, particularly in the field of magnonics [3–6].

One of the critical challenges in utilizing spin waves for practical applications is their dissipation, which limits their lifetime and propagation length. This dissipation is phenomenologically described by the Gilbert damping in the Landau-Lifshitz-Gilbert equation [7]. Yttrium iron garnet (YIG) stands out with the lowest damping constant as low as 10^{-5} , enabling spin wave propagation up to several millimeters [8–10]. The realistic value of the damping constant is influenced by many factors, including the material composition, temperature, and extrinsic geometry or interfaces [11]. For magnonic devices to be viable in information processing, it is essential to enhance spin wave lifetimes and propagation lengths. Consequently, understanding and controlling dissipation has become a central focus in spin wave research.

The vector nature of magnetic moment endows spin waves with a polarization degree of freedom, akin to the polarization in sound and optical waves. The spin wave polarization characteristics differ significantly between ferromagnetic and antiferromagnetic spin waves. In ferromagnets, the broken time-reversal symmetry restricts spin waves to only right-handed circular or elliptical polarization [12]. In contrast, antiferromagnets support both right- and left-handed circular polarizations, as well as their linear combinations, leading to diverse linear and elliptical polarizations [13, 14]. This polarization versatility presents promising opportunities for magnonic information processing based on spin wave polarization manipulation [15–19], offering advantages over traditional methods that rely on amplitude or phase [20–24].

As two important properties of spin wave, dissipation and

polarization are usually considered as distinct phenomena. However, this work reveals a fundamental connection between the two, termed the dissipation-polarization connection. Early in the seventies, Kambersky *et al.* examined the impact of elliptically polarized eigenmodes on ferromagnetic resonance (FMR) linewidth [25], and Puzskarski proposed that elliptical spin precession modifies resonance line intensity [26]. And more recently, Rozsa *et al.* pointed out a link between polarization and linewidth in soft mode excitations in Skyrmions [27]. Our findings suggest that the connection between spin wave dissipation and polarization transcends the specific cases in the these studies, asserting that spin wave dissipation rate, which is closely related to the linewidth of magnetic resonances, is strictly determined by the averaged polarization. We also point out that this connection between spin wave dissipation and polarization is universal: it applies to both ferromagnetic and antiferromagnetic spin waves across various interactions, including anisotropy, exchange, dipolar interactions, and complex magnetic textures. By establishing the dissipation-polarization connection, we enhance the understanding of both spin wave dissipation and polarization, pointing the way for improving spin wave lifetime and propagation length in magnonic applications.

Dissipation-Polarization Connection - The magnetization dynamics is governed by the Landau-Lifshitz-Gilbert equation [7]

$$\dot{\mathbf{m}} = -\gamma \mathbf{m} \times \mathbf{H}_{\text{eff}} + \alpha \mathbf{m} \times \dot{\mathbf{m}}, \quad (1)$$

where γ is gyromagnetic ratio, and α is the Gilbert damping parameter characterizing the dissipation. $\mathbf{H}_{\text{eff}} = -\delta F/\delta \mathbf{m}$ is the effective magnetic field derived from the free energy F . The resonant and dissipative behavior of spin wave mode can be characterized by its complex frequency ω , whose real and imaginary parts represent the resonance frequency and the broadening (linewidth), respectively. We define the magnetic dissipation rate as the ratio of the linewidth to the frequency:

$$\beta \equiv \frac{\text{linewidth}}{\text{peak frequency}} = \frac{\text{Im}\{\omega\}}{|\text{Re}\{\omega\}|}. \quad (2)$$

Patton pointed out that the frequency-swept linewidths, not

field-swept linewidths, are proportional to the dissipation rate [28]. The dissipation rate also characterizes the number of precession cycles before the spin wave is damped out, or the fraction of energy dissipated per cycle. In most common case, the damping rate equals to the Gilbert damping constant, *i.e.* $\beta = \alpha$. In the more general case as discussed in this paper, they are not identical, but $\beta \geq \alpha$.

Because all free energy contributions under consideration are quadratic in \mathbf{m} , for an eigen mode with damping neglected, the tip of the magnetization vector follows along an elliptical trajectory in the complex plane formed by m_x and m_y . This elliptical trajectory can be decomposed as a superposition of right- and left-handed motion: $\psi(t) = m_x + im_y = m^+ e^{i\omega t} + m^- e^{-i\omega t}$, with m^\pm the corresponding (complex) amplitudes. The lengths of semi-axis along the two principal axes of the elliptical trajectory are $a = |m^+| + |m^-|$ and $b = |m^+| - |m^-|$, respectively. And the spin wave polarization can be quantified by the signed ellipticity

$$\eta = \frac{|m^+| - |m^-|}{|m^+| + |m^-|} = \frac{b}{a} \in [-1, 1], \quad (3)$$

for which $\eta > 0$, $\eta < 0$, and $\eta = 0$ correspond to the right-handed, left-handed polarizations, and linearly polarized along the major axis respectively. We may also reparameterize the ellipticity η with a complex parameter r with $\eta = e^{-2r}$, for which real r corresponds to right-handed polarization and r with $\arg r = \pi/2$ corresponds to left-handed one.

The dissipation rate and the polarization are seemingly disconnect concepts. However, for linearized spin wave excitations, we now establish a simple but universal connection between them for the eigenmodes (proof in Appendix A):

$$\beta = \alpha \frac{\eta + \eta^{-1}}{2} = \alpha \cosh(2r). \quad (4)$$

Because $|\cosh(2r)| > 1$, it is evident that the damping rate $|\beta|$ always exceeds the intrinsic Gilbert damping constant α as long as the spin wave is not circular ($|\eta| \neq 1$ or $\text{Re}\{r\} \neq 0$). A simple message is that elliptically polarized spin wave dissipates faster than the circular one.

In the more general case where the Gilbert damping $\alpha_{\mathbf{x}}$ or the polarization $r_{\mathbf{x}}$ vary in space, the dissipation rate $\beta_{\mathbf{x}} = \alpha_{\mathbf{x}} \cosh(2r_{\mathbf{x}})$ is a function of position and is higher (lower) at locations with more elliptical (circular) polarizations. Consequently, the overall dissipation rate of the whole system is given by a weighted average (proof in Appendix A):

$$\beta = \langle \beta_{\mathbf{x}} \rangle \equiv \frac{\int d^3\mathbf{x} S_{\mathbf{x}} \alpha_{\mathbf{x}} \cosh(2r_{\mathbf{x}})}{\int d^3\mathbf{x} S_{\mathbf{x}}}. \quad (5)$$

Since b might take either sign, the weight $S_{\mathbf{x}} = \pi ab = (\pi/\omega) \text{Im}\{\psi(t)\psi^*(t)\}$ here is the directed (signed) area of enclosed by the local magnetization precession trajectory at position \mathbf{x} , and the sign is determined by precession direction (+ for right-handed and - for left-handed). The dissipation-polarization connection in Eq. (5) is exact for linearized spin

wave, *i.e.* the full Hamiltonian is of quadratic form of local magnon creation and annihilation operators, regardless of the types of interactions included. A similar expression to Eq. (5) has been proposed by Rozsa et al. [27] to explain the damping enhancement in non-collinear spin configurations, particularly in ferromagnetic Skyrmions. However, the formulation presented in Eq. (5), which incorporates negative weights for the first time, emerges as a general principle that links dissipation and polarization. This connection is applicable across diverse scenarios, including those where both right-handed and left-handed excitations coexist.

We now verify the polarization-dissipation connection Eq. (5) through several concrete examples, including coupled macrospins, magnetic domain walls, magnetic Skyrmions, and dipolar spin waves. Furthermore, we shall also demonstrate that this connection is not limited to ferromagnetic spin waves, but also applicable to antiferromagnetic spin waves. All simulation results in this paper are carried out using the micromagnetic module that we developed based on COMSOL Multiphysics, which has been applied to simulate ferromagnetic and antiferromagnetic spin waves in both time [16, 18, 29–31] and frequency domain [32].

Coupled Macrospins - We consider a simple system consisting of two macrospins with free energy

$$F = -\frac{K}{2} \sum_{i=1,2} (\mathbf{m}_i \cdot \hat{\mathbf{z}})^2 + \frac{K'}{2} (\mathbf{m}_2 \cdot \hat{\mathbf{y}})^2 - J \mathbf{m}_1 \cdot \mathbf{m}_2, \quad (6)$$

where K is the uniaxial easy axis anisotropy along $\hat{\mathbf{z}}$, K' is the hard-axis anisotropy along $\hat{\mathbf{y}}$, and J is the Heisenberg exchange coupling. The equilibrium magnetization of both sites point in $\hat{\mathbf{z}}$: $\mathbf{m}_1^0 = \mathbf{m}_2^0 = \hat{\mathbf{z}}$. Both macrospins have the same Gilbert damping parameter α . Fig. 1(a) shows the real and imaginary eigenfrequencies of the two-macrospin system as function of the coupling strength J , along with magnetization trajectories for the two macrospins. At $J = 0$, the mode 1, localized on \mathbf{m}_1 , has perfect circular polarization, thus its dissipation rate equals to α . While, the mode 2, localized on \mathbf{m}_2 , has an elliptical polarization because of the additional hard-axis anisotropy, thus its dissipation rate is enhanced as given by Eq. (4). As J becomes non-zero and positive (ferromagnetic coupling), the eigenmodes are no longer localized but encompass both macrospins. In the mean time, mode 1 (2) becomes more (less) elliptical. The dissipation rates calculated from the complex eigenfrequencies (curves in the lower panel of Fig. 1(a)) are in perfect agreement with the rates inferred from the polarization-dissipation connection Eq. (5) (points in lower panel of Fig. 1(a)) based on the spin wave profiles given in right panel of Fig. 1(a).

Bipartite Antiferromagnet - Not only does the dissipation-polarization connection apply to ferromagnetic systems, but it also holds for antiferromagnetic systems. By letting let $J > 0$, $K' = 0$ in Eq. (6), we extend the coupled macrospin model above to the case of antiferromagnetic configuration with $\mathbf{m}_1^0 = -\mathbf{m}_2^0 = \hat{\mathbf{z}}$. The complex frequencies for the antiferromagnetic eigenmodes are [33, 34] $\omega_{\pm} = \pm\sqrt{K(K+2J)} +$

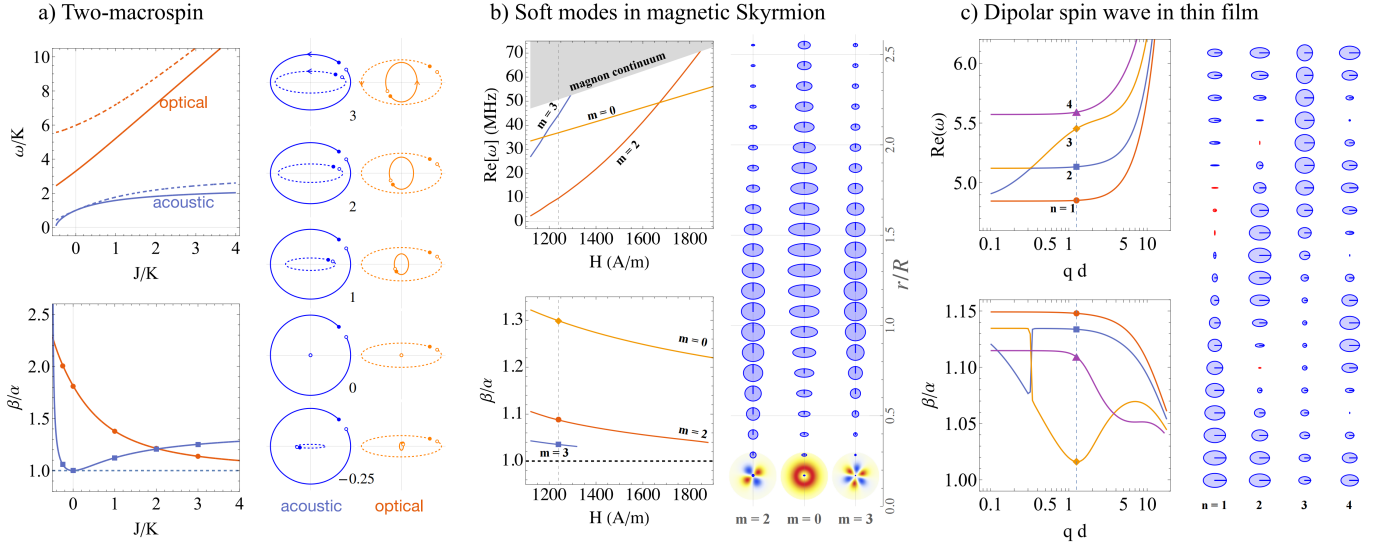


Figure 1. The simulated eigenfrequencies, dissipation rates, and spin wave profiles. (a) The acoustic and optical modes in the two-macrospin model. Top panel: The real (solid) and imaginary (dashed, enlarged by $1/\alpha$) part of the eigenfrequencies for as function of exchange coupling J . Bottom panel: dissipation rates obtained from the dispersions via Eq. (2) (curves) and inferred from the spin wave profiles via Eq. (5) (points). Profile panel: The trajectories on m_x - m_y projection for \mathbf{m}_1 (solid) and \mathbf{m}_2 (dashed) for $J/K = -0.25, 0, 1, 2, 3$. (b) Same as (a) but for the soft modes in Skyrmion. The profiles (at $H = 1240$ A/m) are along the radial direction. (c) Same as (a) but for the dipolar spin wave in tangentially magnetized magnetic thin film with $\mathbf{q} \perp \mathbf{m}_0$ and thickness $d = 305$ nm. The profiles are along the film thickness direction (at $qd = 1.25$). Blue and red orbits correspond to the right-handed and left-handed polarizations. The size of the ellipses is proportional to the square root of the real spin wave amplitudes. In all cases, $\alpha = 0.01$.

$i\alpha(K + J)$. And the dissipation rates are [34]

$$\beta = \alpha \frac{K + J}{\sqrt{K(K + 2J)}}, \quad (7)$$

which is larger than the Gilbert damping constant α . This enhancement can be understood using the dissipation-polarization connection in Eq. (5). An important observation for antiferromagnetic spin wave is that the magnetization from the two sublattices undergoes a circular precession with opposite handedness with respect to its local equilibrium magnetization directions: $\eta_1 = -\eta_2 = \pm 1$ for ω_{\pm} mode, and the precession cone angles $\theta_{1,2}$ have a ratio $(\theta_1/\theta_2)_{\pm} = [K + J \pm \sqrt{K(K + 2J)}]/J$ [33]. Take the ω_+ mode as an example, the opposite precession handedness means $\cosh(2r_1) = +1$ and $\cosh(2r_2) = -1$, and the directed area for the circular orbits of \mathbf{m}_1 and \mathbf{m}_2 are: $S_1 = +\pi\theta_1^2$ and $S_2 = -\pi\theta_2^2$, respectively. Therefore, according to Eq. (5), the weighted polarization $\langle \cosh(2r) \rangle$ is

$$\frac{(+1) \times (+\pi\theta_1^2) + (-1) \times (-\pi\theta_2^2)}{(+\pi\theta_1^2) + (-\pi\theta_2^2)} = \frac{K + J}{\sqrt{K(K + 2J)}},$$

identical to the enhancement factor in Eq. (7), confirming the dissipation-polarization connection in antiferromagnet.

Domain wall - The dissipation-polarization connection also applies to spin wave excitations in complex magnetic textures. An interesting case is the spin wave excitation in a magnetic domain wall with the magnetization rotating from one direction to another. One might anticipate that the inherently

non-collinear structure of the domain wall would lead to an elliptical polarization of the spin waves, thus the dissipation rate would surpass the Gilbert damping constant. Contrary to this expectation, numerical simulations show that the linewidth of spin wave excitation in a magnetic domain wall is identical to the Gilbert damping constant. This intriguing finding indicates that, according to the dissipation-polarization connection Eq. (5), the polarization of the spin wave remains perfectly circular as it traverses the domain wall.

Ferromagnetic Skyrmion - We now consider a ferromagnetic Skyrmion in the magnetic thin film with free energy

$$F = \int d^2\mathbf{r} \left[-\frac{K}{2}(\mathbf{m} \cdot \hat{\mathbf{z}})^2 + \frac{A}{2}(\nabla\mathbf{m})^2 - \frac{D}{2}\mathbf{m} \cdot (\nabla \times \mathbf{m}) - B\mathbf{m} \cdot \hat{\mathbf{z}} \right]. \quad (8)$$

Here, we focus on the soft modes excitation in Skyrmion, including breathing, translational, and rotational modes. We do not anticipate these soft modes to possess circular polarization due to the inherent complexity of this non-collinear structure. Fig. 1(b) shows the simulated results for the eigenfrequencies, the dissipation rates, and the corresponding spin wave profiles as function of external field B applied perpendicular to the film. The dissipation rates β/α (obtained by Eq. (2)) shown as curves in the lower panel of Fig. 1(b) are all greater than the Gilbert damping constant α , implying the non-circular polarization for these modes (the right panel of Fig. 1(b)). The dissipation rates inferred from the spin wave profiles are shown as the points in the lower panel of Fig. 1(b). The exact agree-

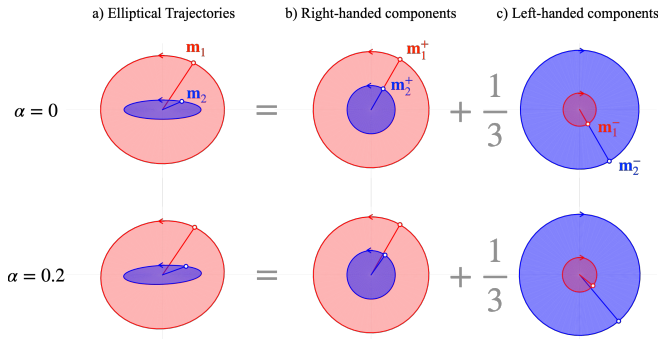


Figure 2. The magnetization trajectory for $\psi(t)$ in complex plane for the two-macrospin model. Left: The overall trajectory $\psi_{1,2}(t)$ for \mathbf{m}_1 (red) and \mathbf{m}_2 (blue). Middle: The right-handed component of the trajectory. Right: The left-handed component (enlarged by three times). The top row with $\alpha = 0$ shows no phase delay between two macrospins, and the bottom row with $\alpha = 0.2$ has a phase delay.

ment confirms the applicability of the dissipation-polarization connection Eq. (5) on the spin wave excitations with spatially varying amplitudes and ellipticities.

Dipolar-exchange spin wave - The dissipation-polarization connection is not limited to local interactions such as the exchange interactions, but also applies to the non-local long range interactions such as the dipole-dipole interaction. The dipolar interaction is intrinsically non-isotropic, leading to non-circular polarization. We now consider the well studied dipolar-exchange spin wave in ferromagnetic thin films [35], but we re-exam it from the viewpoint of its polarization and dissipation rate. We focus on the Damon-Eshbach mode with the equilibrium magnetization lying in the film plane and wave vector perpendicular to the magnetization. The simulated dispersion, dissipation rates (via Eq. (2)), and the spin wave profiles are shown in Fig. 1(c). Since all profiles are elliptically polarized, according to the dissipation-polarization connection Eq. (5), we immediately conclude that their dissipation rates shall all exceed α , as seen in the lower panel of Fig. 1(c). The points in the lower panel of Fig. 1(c) are the dissipation rates inferred from the dissipation-polarization connection Eq. (5) based on the spin wave profiles. They match perfectly with the dissipation rates obtained from the dispersions via Eq. (2). What's especially interesting for the dipolar-exchange spin wave is that the local precession can be even left-handed in a homogeneous ferromagnet [36]: the red profiles for modes $n = 1, 2$ indicating the left-handed motion. Because of this opposite polarization, the integral variable in the denominator of Eq. (5) is partly negative in these left-handed precession locations. The accounting of the signed weights is crucial for the agreement between dissipation rates obtained from dispersions Eq. (2) and via the dissipation-polarization connection Eq. (5) for such situations.

Discussion - In the examples shown above, we observe that the spin wave polarization varies spatially, indicating that the dissipation rates also change across space in accordance with the dissipation-polarization connection Eq. (4). However, for

an eigenmode to maintain its relative profile over time, the dissipation must occur uniformly. This contradiction is resolved by a net energy flow from regions with lower dissipation rate to regions with higher rate, that is the fast-damping region helps dissipate part of the energy in the slow-damping region. In the (collinear) two-macrospin example above, such dissipation energy transfer is calculated by the energy transfer due to the exchange interaction over one period (see Appendix B):

$$J \int_0^T dt \dot{\mathbf{m}}_1 \cdot \mathbf{m}_2 \propto \text{Im} \left\{ m_1^+ m_2^{+*} - m_1^- m_2^{-*} \right\}. \quad (9)$$

This average energy transfer should vanish when Gilbert damping is turned off, indicating that the phase difference between the complex amplitudes at different locations must be either zero or π : $\arg m_1^\pm - \arg m_2^\pm = 0, \pi$ (see top row in Fig. 2 for the case of 0). However, when Gilbert damping is turned on, the trajectories are modulated so that these amplitudes develops a small but critical phase difference $\arg m_1^\pm - \arg m_2^\pm \propto \alpha$ (see bottom row in Fig. 2). Consequently, a net energy transfer between the two sites emerges, thus balancing their different dissipation rates. A similar mechanism has been used to explain the enhanced dissipation rate in antiferromagnets by the present authors [34].

Although the dissipation rate is influenced by the polarization of spin waves, it is important to note that this does not alter the Fluctuation-Dissipation Theorem (FDT) [37–39], *i.e.* the dissipation parameter in the FDT is still the original Gilbert damping parameter α , rather than the enhanced rate β . We should also note that in this work we only consider the simplest local dissipation. Whether the dissipation-polarization connection applies to non-local dissipation such as $\mathbf{m}_i \times \dot{\mathbf{m}}_j$ with $i \neq j$ [40–42] requires further analysis.

In conclusion, we have established a universal connection between the dissipation rate and the polarization of spin waves. This connection is exact for linear spin waves, and it holds for a wide range of systems, including ferromagnetic and antiferromagnetic spin waves, as well as spin waves in complex magnetic textures.

Acknowledgements. This work was supported by National Natural Science Foundation of China (Grants No. 12474110), the National Key Research and Development Program of China (Grant No. 2022YFA1403300), the Innovation Program for Quantum Science and Technology (Grant No.2024ZD0300103), and Shanghai Municipal Science and Technology Major Project (Grant No.2019SHZDZX01).

* Corresponding author: xiaojiang@fudan.edu.cn

- [1] D. D. Stancil and A. Prabhakar, *Spin Waves* (Springer, Office, 2009).
- [2] A. V. Chumak, P. Kabos, M. Wu, C. Abert, C. Adelman, A. Adeyeye, J. Åkerman, F. G. Aliev, A. Anane, A. Awad, C. H. Back, A. Barman, G. E. W. Bauer, M. Becherer, E. N. Beginin, V. A. S. V. Bittencourt, Y. M. Blanter, P. Bortolotti,

- I. Boventer, D. A. Bozhko, S. Bunyaev, J. J. Carmiggelt, R. R. Cheenikundil, F. Ciubotaru, S. Cotofana, G. Csaba, O. Dobrovolskiy, C. Dubs, M. Elyasi, K. G. Fripp, H. Fulara, I. A. Golovchanskiy, C. Gonzalez-Ballester, P. Graczyk, D. Grundler, P. Gruszecki, G. Gubbiotti, K. Guslienko, A. O. Haldar, S. Hamdioui, R. Hertel, B. Hillebrands, T. Hioki, A. Houshang, C.-M. Hu, H. Huebl, M. Huth, E. N. Iacocca, M. B. Jungfleisch, G. Kakazei, A. Khitun, R. Khymyn, T. Kikkawa, M. Kläui, O. Klein, J. W. Klos, S. Knauer, S. Kortalan, M. Kostylev, M. Krawczyk, I. N. Krivorotov, V. V. Kruglyak, D. Lachance-Quirion, S. Ladak, R. Lebrun, Y. Li, M. Lindner, R. Macêdo, G. A. Melkov, S. Mieszczak, Y. Nakamura, H. Nembach, A. A. Nikitin, S. A. Nikitov, V. Novosad, J. Otalora, Y. Otani, A. Papp, B. Pigeau, P. Pirro, W. Porod, F. Porrati, H. Qin, B. Rana, T. Reimann, F. Riente, O. Romero-Isart, A. Ross, A. V. Sadovnikov, E. Saitoh, G. Schmidt, H. Schultheiss, K. Schultheiss, A. A. Serga, S. Sharma, J. Shaw, D. Suess, O. Surzhenko, K. Szulc, T. TANIGUCHI, M. Urbánek, K. Usami, A. B. Ustinov, T. Van Der Sar, S. Van Dijken, V. I. Vasyuchka, R. Verba, S. V. Kusminskiy, Q. Wang, M. Weides, M. Weiler, S. P. Wolski, and X. Zhang, Roadmap on spin-wave computing concepts, *IEEE Transactions on Quantum Engineering* (2021), publisher: IEEE.
- [3] S. O. Demokritov and A. N. Slavin, *Magnonics: From Fundamentals to Applications* (Springer Science & Business Media, 2012) 00000.
- [4] H. Yu, J. Xiao, and H. Schultheiss, Magnetic texture based magnonics, *Physics Reports* **905**, 1 (2021).
- [5] H. Yuan, Y. Cao, A. Kamra, R. A. Duine, and P. Yan, Quantum magnonics: When magnon spintronics meets quantum information science, *Physics Reports* **965**, 1 (2022).
- [6] B. Zare Rameshti, S. Viola Kusminskiy, J. A. Haigh, K. Usami, D. Lachance-Quirion, Y. Nakamura, C.-M. Hu, H. X. Tang, G. E. W. Bauer, and Y. M. Blanter, Cavity magnonics, *Physics Reports Cavity Magnonics*, **979**, 1 (2022).
- [7] T. Gilbert, A phenomenological theory of damping in ferromagnetic materials, *Magnetics, IEEE Transactions on* **40**, 3443 (2004).
- [8] S. Maendl, I. Stasinopoulos, and D. Grundler, Spin waves with large decay length and few 100 nm wavelengths in thin yttrium iron garnet grown at the wafer scale, *Applied Physics Letters* **111**, 012403 (2017).
- [9] H. Qin, S. J. Hämäläinen, K. Arjas, J. Witteveen, and S. van Dijken, Propagating spin waves in nanometer-thick yttrium iron garnet films: Dependence on wave vector, magnetic field strength, and angle, *Physical Review B* **98**, 224422 (2018).
- [10] G. Schmidt, C. Hauser, P. Trempler, M. Paleschke, and E. T. Papaioannou, Ultra Thin Films of Yttrium Iron Garnet with Very Low Damping: A Review, *physica status solidi (b)* **257**, 1900644 (2020).
- [11] S. Azzawi, A. T. Hindmarch, and D. Atkinson, Magnetic damping phenomena in ferromagnetic thin-films and multilayers, *Journal of Physics D: Applied Physics* **50**, 473001 (2017).
- [12] A. G. Gurevich and G. A. Melkov, *Magnetization Oscillations and Waves* (CRC Press, Boca Raton, 1996).
- [13] E. V. Gomonay and V. M. Loktev, Spintronics of antiferromagnetic systems (Review Article), *Low Temperature Physics* **40**, 17 (2014).
- [14] J. Lan, W. Yu, and J. Xiao, Antiferromagnetic domain wall as spin wave polarizer and retarder, *Nature Communications* **8**, 178 (2017).
- [15] R. Cheng, M. W. Daniels, J.-G. Zhu, and D. Xiao, Antiferromagnetic Spin Wave Field-Effect Transistor, *Scientific Reports* **6**, 24223 (2016).
- [16] J. Lan, W. Yu, and J. Xiao, Antiferromagnetic domain wall as spin wave polarizer and retarder, *Nature Communications* **8**, 178 (2017).
- [17] W. Yu, J. Lan, and J. Xiao, Polarization-selective spin wave driven domain-wall motion in antiferromagnets, *Physical Review B* **98**, 144422 (2018).
- [18] W. Yu, J. Lan, and J. Xiao, Magnetic Logic Gate Based on Polarized Spin Waves, *Physical Review Applied* **13**, 024055 (2020).
- [19] J. Han, P. Zhang, Z. Bi, Y. Fan, T. S. Safi, J. Xiang, J. Finley, L. Fu, R. Cheng, and L. Liu, Birefringence-like spin transport via linearly polarized antiferromagnetic magnons, *Nature Nanotechnology*, 1 (2020), publisher: Nature Publishing Group.
- [20] M. P. Kostylev, A. A. Serga, T. Schneider, B. Leven, and B. Hillebrands, Spin-wave logical gates, *Applied Physics Letters* **87**, 153501 (2005).
- [21] T. Schneider, A. A. Serga, B. Leven, B. Hillebrands, R. L. Stamps, and M. P. Kostylev, Realization of spin-wave logic gates, *Applied Physics Letters* **92**, 022505 (2008).
- [22] V. V. Kruglyak, S. O. Demokritov, and D. Grundler, Magnonics, *Journal of Physics D: Applied Physics* **43**, 264001 (2010).
- [23] A. Khitun and K. L. Wang, Non-volatile magnonic logic circuits engineering, *Journal of Applied Physics* **110**, 034306 (2011).
- [24] A. Mahmoud, F. Ciubotaru, F. Vanderveken, A. V. Chumak, S. Hamdioui, C. Adelmann, and S. Cotofana, Introduction to spin wave computing, *Journal of Applied Physics* **128**, 161101 (2020).
- [25] V. Kambarsky and C. E. Patton, Spin-wave relaxation and phenomenological damping in ferromagnetic resonance, *Physical Review B* **11**, 2668 (1975), publisher: American Physical Society.
- [26] H. Puszkarski, Theory of surface states in spin wave resonance, *Progress in Surface Science* **9**, 191 (1979).
- [27] L. Rózsa, J. Hagemester, E. Y. Vedmedenko, and R. Wiesendanger, Effective damping enhancement in noncollinear spin structures, *Physical Review B* **98**, 100404 (2018), publisher: American Physical Society.
- [28] C. E. Patton, Linewidth and Relaxation Processes for the Main Resonance in the Spin-Wave Spectra of Ni-Fe Alloy Films, *Journal of Applied Physics* **39**, 3060 (1968).
- [29] J. Lan, W. Yu, R. Wu, and J. Xiao, Spin-Wave Diode, *Physical Review X* **5**, 041049 (2015).
- [30] W. Yu, J. Lan, and J. Xiao, Polarization-selective spin wave driven domain-wall motion in antiferromagnets, *Physical Review B* **98**, 144422 (2018).
- [31] W. Yu, J. Xiao, and G. E. W. Bauer, Hopfield neural network in magnetic textures with intrinsic Hebbian learning, *Physical Review B* **104**, L180405 (2021), publisher: American Physical Society.
- [32] J. Zhang, W. Yu, X. Chen, and J. Xiao, A frequency-domain micromagnetic simulation module based on COMSOL Multiphysics, *AIP Advances* **13**, 055108 (2023).
- [33] F. Keffer and C. Kittel, Theory of Antiferromagnetic Resonance, *Physical Review* **85**, 329 (1952), 00207.
- [34] Y. Wang and J. Xiao, Mechanism for broadened linewidth in antiferromagnetic resonance, *Physical Review B* **110**, 134409 (2024), publisher: American Physical Society.
- [35] R. E. De Wames and T. Wolfram, Dipole-Exchange Spin Waves in Ferromagnetic Films, *Journal of Applied Physics* **41**, 987 (1970).
- [36] G. Dieterle, J. Förster, H. Stoll, A. S. Semisalova, S. Finizio, A. Gangwar, M. Weigand, M. Noske, M. Fähnle, I. Bykova, J. Gräfe, D. A. Bozhko, H. Y. Musiienko-Shmarova, V. Tiberkevich, A. N. Slavin, C. H. Back, J. Raabe, G. Schütz, and

S. Wintz, Coherent Excitation of Heterosymmetric Spin Waves with Ultrashort Wavelengths, PHYSICAL REVIEW LETTERS (2019).

- [37] L. Onsager, Reciprocal Relations in Irreversible Processes. II., Physical Review **38**, 2265 (1931), copyright (C) 2009 The American Physical Society; Please report any problems to prola@aps.org.
- [38] R. Kubo, The fluctuation-dissipation theorem, Reports on Progress in Physics **29**, 255 (1966).
- [39] W. F. Brown, Thermal Fluctuations of a Single-Domain Particle, Physical Review **130**, 1677 (1963).
- [40] S. Zhang and S. S.-L. Zhang, Generalization of the Landau-Lifshitz-Gilbert Equation for Conducting Ferromagnets, Physical Review Letters **102**, 086601 (2009).
- [41] Y. Tserkovnyak, E. M. Hankiewicz, and G. Vignale, Transverse spin diffusion in ferromagnets, Physical Review B **79**, 094415 (2009).
- [42] H. Y. Yuan, Q. Liu, K. Xia, Z. Yuan, and X. R. Wang, Proper dissipative torques in antiferromagnetic dynamics, EPL (Europhysics Letters) **126**, 67006 (2019).

Relation between magnetic damping and polarization

Consider a discrete system with N sites. The energy function of linearized spin wave is quadratic and can be written as

$$H = \frac{1}{2} \hat{\Psi}^\dagger \begin{pmatrix} A & B \\ B^* & A^* \end{pmatrix} \hat{\Psi} = \frac{1}{2} \hat{\Psi}^\dagger h \hat{\Psi}, \quad (10)$$

where $\hat{\Psi} = (\hat{\psi}_1, \hat{\psi}_2, \dots, \hat{\psi}_N, \hat{\psi}_1^*, \hat{\psi}_2^*, \dots, \hat{\psi}_N^*)^T$ and $\hat{\psi}_j = \delta m_j^{(\theta)} + i \delta m_j^{(\phi)}$ is the local magnon creation operator. It satisfies the commutation relation $[\hat{\psi}_j^*, \hat{\psi}_k] = \delta_{j,k}$ and other commutators are all zero. A is the self-energy and hopping term, and B is the squeezing term. The Heisenberg equation of motion is an eigenvalue problem,

$$-i \frac{d}{dt} \hat{\Psi} = \Sigma_z h \hat{\Psi}, \quad (11)$$

where $\Sigma_z = \sigma_z \otimes I_{N \times N}$ and σ_z and I are the Pauli z matrix and identity matrix, respectively.

We can get the magnon frequencies by solving the equation of motion using Bogoliubov transformation,

$$U^{-1} \Sigma_z h U = \begin{pmatrix} \Lambda & 0 \\ 0 & -\Lambda \end{pmatrix}, \quad (12)$$

with the eigenvectors

$$\hat{\Phi} = U^{-1} \hat{\Psi}. \quad (13)$$

Λ is semi-positive defined diagonal matrix $\Lambda = \text{diag}(\lambda_1, \lambda_2, \dots, \lambda_N)$. We can label eigenvalues in the right below block in sequence. Its index j is larger than N and we have $\lambda_j = -\lambda_{j-N}$. The eigenvalue λ_i , $1 \leq i \leq N$, is nonnegative to ensure the stability of ground state.

The matrix U can be written as

$$U = \begin{pmatrix} M & N \\ N^* & M^* \end{pmatrix}. \quad (14)$$

To ensure the bosonic commutation relation, it is an element of $U(N, N)$,

$$U^\dagger \Sigma_z U = \Sigma_z. \quad (15)$$

It is easy to verify its inverse,

$$U^{-1} = \Sigma_z U^\dagger \Sigma_z = \begin{pmatrix} M^\dagger & -N^T \\ -N^\dagger & M^T \end{pmatrix}. \quad (16)$$

Suppose that the eigenvector of i th eigenvalues λ_i is $|\Phi_i\rangle e^{i\lambda_i t}$. It satisfies the eigenvalue equation,

$$\Sigma_z h |\Phi_i\rangle = \lambda_i |\Phi_i\rangle. \quad (17)$$

Note that the effective Hamiltonian $\Sigma_z h$ is non-Hermitian, the orthonormal relation is different from the Hermitian case,

$$\langle \Phi_i | \Sigma_z | \Phi_j \rangle = (\Sigma_z)_{i,j}. \quad (18)$$

Now consider the effect of Gilbert damping with damping parameter α . $\alpha = \text{diag}(\alpha_1, \alpha_2 \cdots, \alpha_N, \alpha_1, \alpha_2 \cdots, \alpha_N)$ is a diagonal matrix. Different labels of α indicate that the Gilbert damping could be different for different sites. The damping term adds a damping matrix to the equation of motion

$$-i(1 - i\alpha\Sigma_z) \frac{d}{dt} \hat{\Psi} = \Sigma_z h \hat{\Psi}. \quad (19)$$

It is still a eigenvalue problem,

$$-i \frac{d}{dt} \hat{\Psi} = (1 - i\alpha\Sigma_z)^{-1} \Sigma_z h \hat{\Psi} = (\Sigma_z h + i\alpha h + O(\alpha^2)) \hat{\Psi}. \quad (20)$$

We don't need to solve the whole problem. Treat α as a small number, we are interested in the first order correction of the eigenvalues λ_i . The zeroth order correction is λ_i itself $\lambda_i^{(0)} = \lambda_i$. The first order correction is given by perturbation theory, for $i \leq N$,

$$\lambda_i^{(1)} = i \langle \Phi_i | \Sigma_z | \alpha h | \Phi_i \rangle = i \lambda_i^{(0)} \langle \Phi_i | \alpha | \Phi_i \rangle. \quad (21)$$

For $N < i \leq 2N$, the first order correction is similar,

$$\lambda_i^{(1)} = -i \lambda_i^{(0)} \langle \Phi_i | \alpha | \Phi_i \rangle = i |\lambda_i^{(0)}| \langle \Phi_i | \alpha | \Phi_i \rangle. \quad (22)$$

We just need to focus on the first N states, because the other N states have the same decay rates with their conjugation partners. The eigenfrequency with damping considered is then $\omega_i = \lambda_i + i \lambda_i \langle \Phi_i | \alpha | \Phi_i \rangle$ for $1 \leq i \leq N$. The ratio between the imaginary part and the real part of ω_i gives the β parameter,

$$\beta_i = \frac{\text{Im}\{\omega_i\}}{\text{Re}\{\omega_i\}} = \langle \Phi_i | \alpha | \Phi_i \rangle. \quad (23)$$

If the normalization of eigenvectors isn't strictly guaranteed, which is always the case in practice, we need to divide the metric norm of vector when getting the first order correction,

$$\lambda_i^{(1)} = i \frac{\langle \Phi_i | \alpha | \Phi_i \rangle}{\langle \Phi_i | \Sigma_z | \Phi_i \rangle} \lambda_i^{(0)}. \quad (24)$$

Thus, the β parameter is

$$\beta_i = \frac{\langle \Phi_i | \alpha | \Phi_i \rangle}{\langle \Phi_i | \Sigma_z | \Phi_i \rangle}. \quad (25)$$

Now parametrize the eigenvector $|\Phi_i\rangle$ as $|\Phi_i\rangle = (M_{1,i}, M_{2,i}, \cdots, M_{N,i}, N_{1,i}^*, N_{2,i}^*, \cdots, N_{N,i}^*)^T$. Then, the metric norm is

$$\langle \Phi_i | \Sigma_z | \Phi_i \rangle = \sum_{j=1}^N |M_{j,i}|^2 - |N_{j,i}^*|^2. \quad (26)$$

The β parameter can be written as

$$\beta_i = \frac{\sum_{j=1}^N \alpha_j (|M_{j,i}|^2 + |N_{j,i}^*|^2)}{\sum_{j=1}^N |M_{j,i}|^2 - |N_{j,i}^*|^2}. \quad (27)$$

The time evolution of the j th sites can be extracted from the Bogoliubov transformation Eq. (13). If the system is in the coherent state of k th mode at $t = 0$, $\hat{\Phi}_k |\xi\rangle = \xi |\xi\rangle$, the time evolution of the j th site is

$$\langle \psi_j(t) \rangle = M_{j,k} \xi^* e^{i\lambda_k t} + N_{j,k} \xi e^{-i\lambda_k t}. \quad (28)$$

We may assume ξ to be real, since its argument can be absorbed into the $e^{i\lambda_k t}$ term. The real part and imaginary parts of $\langle \psi_j \rangle$ correspond to two orthogonal components of the local magnon field. The trajectory of $\langle \psi_j(t) \rangle$ is an ellipse on complex plane with its center on the origin. We label the lengths of semi-major axis and semi-minor axis as a_j and b_j respectively. The trajectory can be parametrized as

$$\langle \psi_j(t) \rangle = e^{i\theta_j} [a_j \cos(\lambda_k t + \phi_j) + ib_j \sin(\lambda_k t + \phi_j)], \quad (29)$$

$$a_j = \xi (|M_{j,k}| + |N_{j,k}|), \quad (30a)$$

$$b_j = \xi (|M_{j,k}| - |N_{j,k}|), \quad (30b)$$

$$\theta_j = \frac{1}{2} \arg(M_{j,k} N_{j,k}) \quad (30c)$$

$$\phi_j = \frac{1}{2} \arg(M_{j,k} N_{j,k}^*). \quad (30d)$$

We can verify that $a_j^2 + b_j^2 = 2\xi^2 (|M_{j,k}|^2 + |N_{j,k}|^2)$ and $a_j b_j = \xi^2 (|M_{j,k}|^2 - |N_{j,k}|^2)$. Note that for $|M_{j,k}| > |N_{j,k}|$, we have $a_j > b_j > 0$ and the precession is right-handed. For $|M_{j,k}| < |N_{j,k}|$, we have $a_j > 0 > b_j$ and the precession is left-handed.

If we define a signed area of the ellipse, $S_j = \pi a_j b_j$ based on the precession direction of local magnon. For right-handed precession, $a_j > b_j > 0$, we have positive area $S_j > 0$. For left-handed precession, $a_j > 0 > b_j$, we have negative area $S_j < 0$. Then, we can calculate the β parameter based on the ellipse trajectory of each site,

$$\beta = \frac{\sum_{j=1}^N \alpha_j (a_j^2 + b_j^2)}{\sum_{j=1}^N 2a_j b_j}. \quad (31)$$

Recall that $\eta = \frac{b}{a} = e^{-2r}$ in the main text. We can rewrite the numerator with η ,

$$a_j^2 + b_j^2 = a_j b_j (\eta + \eta^{-1}) = 2a_j b_j \cosh(2r_j). \quad (32)$$

Note that, for left-handed precession sites, $\cosh(2r_j)$ is negative and the whole numerator $a_j b_j \cosh(2r)$ is still positive. Finally, we get the β parameter,

$$\beta = \frac{\sum_{j=1}^N \pi \alpha_j a_j b_j \cosh(2r_j)}{\sum_{j=1}^N \pi a_j b_j} = \frac{\sum_{j=1}^N S_j \alpha_j \cosh(2r_j)}{\sum_{j=1}^N S_j}. \quad (33)$$

For a single site, we don't need the summation. The weight S_j is then cancel out, $\beta = \alpha \cosh(2r)$. In continuous limit, the summation becomes an integral,

$$\beta = \frac{\int d^3\mathbf{x} S_{\mathbf{x}} \alpha_{\mathbf{x}} \cosh(2r_{\mathbf{x}})}{\int d^3\mathbf{x} S_{\mathbf{x}}}.. \quad (34)$$

We get the Eq. (5) in the main text.

Phase delay induced energy flow

The Gilbert damping is local and related to the polarization of the local spin, *i.e.* $\alpha \cosh(2r)$. While the system shares the same damping rate in eigenstate. The polarization of different place is different, which means that the energy loss rate by Gilbert damping is different, so there should be another mechanism to balance this difference.

Consider the two-macrospin model as an example. The free energy is

$$F = -\frac{K}{2} \sum_{i=1,2} (\mathbf{m}_i \cdot \hat{\mathbf{z}})^2 + \frac{K'}{2} (\mathbf{m}_2 \cdot \hat{\mathbf{y}})^2 - J \mathbf{m}_1 \cdot \mathbf{m}_2. \quad (35)$$

The effective fields for lattice 1 and 2 are

$$\begin{aligned} H_1 &= K(\mathbf{m}_1 \cdot \hat{\mathbf{z}})\hat{\mathbf{z}} + J\mathbf{m}_2 \\ H_2 &= K(\mathbf{m}_2 \cdot \hat{\mathbf{z}})\hat{\mathbf{z}} - K'(\mathbf{m}_2 \cdot \hat{\mathbf{y}})\hat{\mathbf{y}} + J\mathbf{m}_1. \end{aligned} \quad (36)$$

The ground state is a ferromagnet $\mathbf{m}_{10} = \mathbf{m}_{20} = \hat{\mathbf{z}}$. Consider the spin wave excitation around ground state $\delta\mathbf{m}_i = \mathbf{m}_i - \mathbf{m}_{i0} \approx (m_i^x, m_i^y, 0)$ and $|\delta\mathbf{m}_i| \ll 1$. With the help of complex combination $\psi_j = m_j^x + im_j^y$, we can write the linearized LLG equation,

$$\begin{aligned} -i(1 - i\alpha_1)\dot{\psi}_1 &= (K + J)\psi_1 - J\psi_2, \\ -i(1 - i\alpha_2)\dot{\psi}_2 &= (K + J)\psi_2 + \frac{K'}{2}(\psi_2 - \psi_2^*) - J\psi_1. \end{aligned} \quad (37)$$

The solutions of these equations give ellipse trajectories $\psi_j = m_j^+ e^{i\omega t} + m_j^- e^{-i\omega t}$ with the lengths of two principal axes a_j and b_j .

When the damping is neglected, the tangent direction of the trajectory is $\dot{\mathbf{m}}_j$ and $\mathbf{m}_{j0} \cdot (\dot{\mathbf{m}}_j \times \boldsymbol{\tau})$ gives the area decrease due to the torque $\boldsymbol{\tau}$ in time $t \sim t + dt$. The linearized form under complex combination is $\text{Im}(\dot{\psi}_j \tau^*)$. The integral average of the ratio of $\text{Im}(\dot{\psi}_j \tau^*)$ and its trajectory area over one period give the total relative decrease

$$\mathcal{A}_j(\tau) = \frac{\omega}{2\pi} \int_0^{2\pi/\omega} \frac{\text{Im}(\dot{\psi}_j \tau^*)}{a_j b_j \omega} dt. \quad (38)$$

If damping is considered, the eigenfrequency gets an imaginary part $\text{Re}\{\omega\} = \omega_0$ and $\text{Im}\{\omega\} = \omega'$. The ellipse shrinks and the lengths of two axes decrease exponentially $a_j(t) = a_j(0)e^{-\omega' t}$. The time derivative of ψ_j compensated with $\omega' \psi_j$ is then on the tangent direction of the ellipse,

$$\mathcal{T}_j = \dot{\psi}_j + \omega' \psi_j. \quad (39)$$

The area decrease is then $\text{Im}(\mathcal{T}_j \tau^*)$. Note that $\text{Im}(\mathcal{T}_j \psi_j^*) = \omega_0 a_j b_j e^{-2\omega' t}$ is proportion to the corresponding ellipse area at time t . The relative area decrease in one period is the integral average of the ratio between them,

$$\mathcal{A}_j(\tau) = \frac{\omega_0}{2\pi} \int_0^{2\pi/\omega_0} \frac{\text{Im}(\mathcal{T}_j \tau^*)}{\text{Im}(\mathcal{T}_j \psi_j^*)} dt. \quad (40)$$

We could examine the terms in LLG equation one by one. The time derivative of ψ_j gives the total damping

$$\mathcal{A}_j(\dot{\psi}_j) = \frac{\omega_0}{2\pi} \int_0^{2\pi/\omega_0} \frac{\text{Im}(\mathcal{T}_j \dot{\psi}_j^*)}{\text{Im}(\mathcal{T}_j \psi_j^*)} dt = -\omega'. \quad (41)$$

The Gilbert damping term $i\alpha_j \dot{\psi}_j$ gives the area loss due to Gilbert damping, *i.e.* the trajectory polarizations,

$$\mathcal{A}_j(i\alpha_j \dot{\psi}_j) = -\alpha_j \omega_0 \frac{a_j^2 + b_j^2}{2a_j b_j} = -\alpha_j \omega_0 \cosh(2r_j). \quad (42)$$

The torque from local anisotropy is a linear composition of ψ_j and ψ_j^* , $\tau_A = iu_1 \psi_j + iu_2 \psi_j^*$, with $u_1 \in \mathbb{R}$ and $u_2 \in \mathbb{C}$. Its contribution to the area loss is always zero

$$\mathcal{A}_j(\tau_A) = 0. \quad (43)$$

The exchange torque from two lattices with collinear ground state is $\tau_E = iJ(\psi_j - \psi_l)$. Its contribution is related to the phase delay of two lattices

$$\mathcal{A}_{jl}(\tau_E) = \frac{J \text{Im}\{m_j^+ m_l^{+*} - m_j^- m_l^{-*}\}}{a_j b_j} \quad (44)$$

$\mathcal{A}(\tau)$ is a linear function, $\mathcal{A}(c_1 \tau_1 + c_2 \tau_2) = c_1 \mathcal{A}(\tau_1) + c_2 \mathcal{A}(\tau_2)$ for $c_1, c_2 \in \mathbb{R}$. Apply it to LLG equations of two macrospin model, we find that

$$\mathcal{A}_1(\dot{\psi}_1) = \mathcal{A}_1(i\alpha_1 \dot{\psi}_1) + \mathcal{A}_{12}(\tau_E). \quad (45)$$

It means that the total area loss is equal to the sum of loss due to Gilbert damping and the transfer between two lattices. We verify this result by examining it on the numerical solution of two macrospin model.

If we compensated the exponential decay part of the eigenvector, we could neglect the denominator since $\text{Im}(e^{2\omega' t} \mathcal{T}_j \psi_j^*) = \omega_0 a_j b_j$ is a constant. Using the compensated eigenstate $\tilde{\psi}_j = e^{\omega' t} \psi_j$, we have $\mathcal{T}_j = e^{-\omega' t} \dot{\tilde{\psi}}_j$ we could define the absolute area loss,

$$\tilde{\mathcal{A}}_j(\tau) = \frac{\omega_0}{2\pi} \int_0^{2\pi/\omega_0} \text{Im}(\dot{\tilde{\psi}}_j \tau^*) dt. \quad (46)$$

The transfer between two lattices could be written as

$$\tilde{\mathcal{A}}_{jl}(\tau_E) = \left\langle \text{Im}\left\{iJ\dot{\tilde{\psi}}_j(\tilde{\psi}_j - \tilde{\psi}_l)^*\right\}\right\rangle = \left\langle \text{Im}\left\{-iJ\dot{\tilde{\psi}}_j \tilde{\psi}_l^*\right\}\right\rangle. \quad (47)$$

Then we have

$$\omega' \omega_0 a_j b_j = \left\langle \alpha_j |\dot{\tilde{\psi}}_j|^2 \right\rangle + \left\langle \text{Im}\left\{iJ\dot{\tilde{\psi}}_j \tilde{\psi}_l^*\right\}\right\rangle. \quad (48)$$

Its physical meaning is the same as above.

Now focus on the Heisenberg exchange transfer term, and suppose \mathbf{m} represents the compensated magnetic vector, we have

$$\begin{aligned}
 \tilde{\mathcal{A}}_{12}(\tau_E) &= -\frac{\omega_0 J}{2\pi} \int_0^{2\pi/\omega_0} \hat{\mathbf{z}} \cdot (\dot{\mathbf{m}}_1 \times (\mathbf{m}_1 \times \mathbf{m}_2)) dt \\
 &= -\frac{\omega_0 J}{2\pi} \int_0^{2\pi/\omega_0} \dot{\mathbf{m}}_1 \cdot \mathbf{m}_2 dt \\
 &= -J \operatorname{Im} \left\{ m_1^+ m_2^{+*} - m_1^- m_2^{-*} \right\}
 \end{aligned} \tag{49}$$

It gives the flow from lattice 1 to lattice 2, which balance the mismatch of area loss from Gilbert damping due to space varies polarization.